NeuroImage: Clinical 25 (2020) 102124

Contents lists available at ScienceDirect

NeuroImage: Clinical

journal homepage: www.elsevier.com/locate/ynicl

Takotsubo syndrome: How the broken heart deals with negative emotions

Carina Klein[a,1,*], Simon Leipold[a,1], Jelena-Rima Ghadri[b], Stjepan Jurisic[b], Thierry Hiestand[b], Jürgen Hänggi[a], Thomas F. Lüscher[e,f], Lutz Jäncke[a,c,d,2], Christian Templin[b,2]

[a] Division Neuropsychology, Department of Psychology, University of Zurich, Binzmühlestrasse 14, Box 25, Zürich CH-8050, Switzerland
[b] University Heart Center, Department of Cardiology, University Hospital Zurich, Zurich, Switzerland
[c] International Normal Aging and Plasticity Imaging Center (INAPIC), University of Zurich, Zurich, Switzerland
[d] University Research Priority Program (URPP), Dynamics of Healthy Aging, University of Zurich, Zurich, Switzerland
[e] Center for Molecular Cardiology, University of Zurich, Switzerland
[f] Imperial College and Royal Brompton & Harefield Hospital, London, United Kingdom

ARTICLE INFO

Keywords:
Broken heart syndrome
Emotion regulation
Picture processing
Brain-heart connection

ABSTRACT

Objectives: Patients suffering from Takotsubo syndrome have a higher prevalence of anxiety and depressive disorders compared to those with acute myocardial infarction and might thus show impaired regulation and processing of emotions.
Methods: In this cross-sectional study, neural activity during an emotional picture processing task was examined in 26 Takotsubo patients (on average 27 months after the Takotsubo event) and 22 healthy age- and gender-matched control subjects undergoing functional magnetic resonance imaging. Imaging data were analyzed with two complementary approaches: First, univariate analysis was used to detect brain regions showing condition-specific differences in mean neural activity between groups. Second, multivariate pattern analysis was applied to decode the experimental conditions from individual activity patterns.
Results: In the univariate analysis approach, patients showed lower bilateral superior parietal activity during the processing of negative expected pictures compared to the control subjects. The multivariate pattern analysis revealed group differences in decoding negative versus neutral pictures from a widespread network consisting of frontal, parietal, occipital, and cerebellar brain regions. Additionally, differences in decoding the expectation of a negative versus positive upcoming picture were observed in the visual cortex.
Conclusion: The lower involvement of brain regions observed in Takotsubo patients suggests an impairment in emotion regulation, which might be of etiological importance in this brain-heart disease.

1. Introduction

Stress is a psychological process most often initiated by external circumstances. It has a major influence on behavior, well-being, and even human health in today's society. Research has shown that psychological stress produces a range of physiological changes, which might contribute to the development of cardiovascular diseases (Steptoe and Kivimaki, 2012).

Takotsubo syndrome, which is also known as stress cardiomyopathy, or broken heart syndrome, is characterized by acute left ventricular dysfunction occurring mainly in post-menopausal women (Templin et al., 2015). On admission, Takotsubo patients show signs and symptoms similar to acute myocardial infarction, such as chest pain, dyspnea, electrocardiographic anomalies, and changes in cardiac biomarkers (Ghadri et al., 2018a; Jaguszewski et al., 2014). However, in contrast to patients with classical heart attacks, the majority of Takotsubo patients do not have a culprit coronary lesion that is responsible for the wall motion abnormalities of the left ventricle seen in Takotsubo syndrome (Napp et al., 2015a,b). Notably, the syndrome is often triggered by an acute physical or emotional stressor (Templin et al., 2015). Emotional stressors can be negative or positive in nature (Ghadri et al., 2016). For example, joyful events, such as attending a wedding or birthday party or winning a jackpot are considered to be stressors. In this regard, Takotsubo syndrome has also been coined the “happy heart syndrome” (Ghadri et al., 2016).

These findings gave rise to the idea that Takotsubo syndrome has a

* Corresponding author.
E-mail address: carina.klein@uzh.ch (C. Klein).
[1] These authors contributed equally to this work.
[2] Shared last authorship.

https://doi.org/10.1016/j.nicl.2019.102124
Received 15 October 2019; Received in revised form 5 December 2019; Accepted 13 December 2019
Available online 13 December 2019

stress-induced neurocardiogenic etiology, in which an underlying overactivation of the sympathetic nervous system might lead to an overshoot of catecholamines that finally contributes to myocardial damage (Borchert et al., 2017; Ghadri et al., 2018b; Wittstein et al., 2005). This idea prompted Suzuki et al. (2014) to compare the cerebral blood flow of healthy control subjects and three acute Takotsubo patients over time. The study found that the patients had increased blood flow in subcortical brain regions (hippocampus, basal ganglia, and brain stem) and decreased blood flow in the prefrontal cortex, with the decrease persisting for several weeks. In light of these results, we and others identified brain alterations in chronic Takotsubo patients by using magnetic resonance imaging (MRI) (Hiestand et al., 2018; Klein et al., 2017; Pereira et al., 2016; Sabisz et al., 2016; Templin et al., 2019). On the structural level, Hiestand et al. (2018) discovered a reduced cortical thickness in Takotsubo patients compared to healthy controls in both bilateral insulae and cingulate cortices. A reduced cortical volume was found in the patients in the left and right amygdala as well as in the right hippocampus. Besides regulating autonomic responses, many of the affected brain regions are also involved in the processing and regulation of emotions (Etkin et al., 2015; Hiestand et al., 2018; Lindquist et al., 2012; Pereira et al., 2016). The results of a resting state functional magnetic resonance imaging (fMRI) study showed an altered connectivity in Takotsubo patients compared to healthy control subjects in a frontal network (precuneus and ventromedial prefrontal cortex), suggesting an increased focus on the self, accompanied by a decreased capacity for emotional control (Sabisz et al., 2016). However, this study included only a small number of subjects. Recently, we have reported that structural and functional neuroimaging parameters of the brain regions involved in the limbic and autonomic nervous system may predict Takotsubo syndrome, making it possible to classify a subject as a Takotsubo patient or a healthy control subject (Klein et al., 2017).

To date, only one task-based fMRI case study including only 4 patients has investigated neural activity in Takotsubo patients compared to a healthy control group during a stressful situation (i.e. the Valsalva maneuver, the exhalation against a closed airway) (Pereira et al., 2016). Patients in that case series showed increased activity in the insula, amygdala, and hippocampus during the task. However, these results might be biased because of the low number of patients ($n = 4$). Furthermore, no statistical correction was made for multiple comparisons, which might have led to inflated false-positive rates (Button et al., 2013).

As many of the brain regions reported in Takotsubo patients are involved in the autonomic nervous system as well as in the processing and regulation of emotions, the aim of the present study was to investigate emotional processing in Takotsubo patients and healthy age- and gender matched controls during an emotional picture processing task, while undergoing fMRI scanning. Besides allowing for the analysis of signal changes in the blood oxygenation level dependent (BOLD) response to the emotional pictures (presentation period), this task also allows to distinguish brain activity patterns while expecting an emotional event (expectation period).

2. Materials and methods

2.1. Subjects

Thirty patients (25 women) with the diagnosis of Takotsubo syndrome were enrolled in the study. The inclusion criteria were based on the InterTAK diagnostic criteria (Ghadri et al., 2018a). Twenty-three healthy control subjects (18 women), matched for age, handedness (Annett, 1970) and Mini-Mental State Examination (MMSE) scores (Folstein et al., 1975) also participated in the study. The Takotsubo patients were selected from the International Takotsubo Registry (www.takotsubo-registry.com) of the University Hospital Zurich in Zurich, Switzerland. The subjects' levels of anxiety and depression were assessed with the Hospital Anxiety and Depression Scale (HADS) (Zigmond and Snaith, 1983). Data acquisition took place between July 2013 and September 2015 on a 3T MRI scanner of the University Hospital Zurich, Institute for Biomedical Engineering.

Fourteen of the 25 Takotsubo patients entering data analysis reported to have experienced an emotional triggering event prior to Takotsubo, six patients experienced a physically stressful situation, one patient both types of triggering events, and one patient reported to not have experienced any particular type of stressful event. None of the subjects reported a history of neurological or psychiatric disorders, head injuries, alcohol or drug abuse, or contraindications for MRI. Written informed consent was obtained from all the subjects prior to participation in the study. Four patients were excluded from the study because of an incomplete task ($n = 1$ control group, $n = 3$ patient group). Another Takotsubo patient was excluded from the analyses due to anatomical anomalies. The study was approved by the local ethics committee "Kantonale Ethikkommission Zürich" (www.kek-zh.ch) and conducted according to the principles of the Declaration of Helsinki.

2.2. Experimental procedure

The subjects performed an emotional picture processing task during fMRI scanning (Herwig et al., 2007b). Pictures containing positive, negative, and neutral emotional content were taken from the International Affective Picture System (IAPS; Lang et al., 1995). The pictures were matched for complexity, arousal, and the depiction of natural scenes, faces, and food (Herwig et al., 2007a). All the stimuli were presented with the Presentation software (www.neurobs.com).

The task included 56 trials that fell into five experimental conditions: expected positive pictures (14 trials), expected negative pictures (14 trials), expected neutral pictures (14 trials), unexpected positive pictures (7 trials), and unexpected negative pictures (7 trials). The trials were presented in a randomized order, and this order was kept constant across all the subjects.

Each trial consisted of four consecutive events: During the first 1,000 ms, a small white cue was presented in the center of a black screen; the size of the cue was 1/40 of the screen height. In the three conditions with expected pictures, this cue indicated the valence of the picture that subsequently appeared. A positive symbol ("∪") signaled the appearance of a positive picture, a negative symbol ("∩") signaled the appearance of a negative picture, and a neutral symbol ("–") signaled the appearance of a neutral picture. In the two conditions with unexpected pictures, a fourth symbol ("|") signaled the appearance of a picture of unknown valence to the subject. The meaning of the symbols was explained to the subjects before the fMRI scanning session. A white dot appeared at the center of the screen for 6,920 ms (expectation period) between the presentation of the cues and the pictures. The pictures were presented for 7,920 ms and filled the entire screen (presentation period). After a picture was presented, the white dot in the center of the screen appeared again for 15,840 ms. During this extended period, the BOLD signal was allowed to return to baseline before the start of the next trial. The experimental design implemented in this task can therefore be characterized as a slow event-related design. The complete task had a duration of about 30 min.

2.3. Magnetic resonance imaging data acquisition

Functional and structural images were acquired on a Philips Ingenia 3.0 T MRI system (Philips Medical Systems, Best, the Netherlands), equipped with a commercial 15-channel head coil. Whole-brain functional images were acquired in a single run using a T2*-weighted gradient echo (GRE) echo planar imaging (EPI) single-shot sequence with the following parameters: repetition time (TR): 2.1 s, echo time (TE): 35 ms, flip angle $\alpha = 77°$, sensitivity encoding (SENSE) reduction factor: 2.3, slice scan order: interleaved, number of axial slices: 34, slice thickness: 4 mm (no gap), field of view (FOV): 220 × 220 mm^2,

acquisition voxel size: 2.75 × 2.75 × 4.00 mm^3; reconstructed to a spatial resolution of 1.72 × 1.72 × 4.00 mm^3 with a reconstruction matrix of 128 × 128, number of dummy scans: 3, total number of scans: 920, total scan duration: 32 min. A whole-brain structural image was acquired for each subject using a T1-weighted GRE turbo field echo sequence with the following parameters: TR: 8.1 ms, TE: 3.7 ms, flip angle $\alpha = 8^{\circ}$, SENSE reduction factor: 1.5, number of sagittal slices = 160, FOV: 240 × 240 mm^2, acquisition voxel size: 1.0 × 1.0 × 1.0 mm^3; reconstructed to a spatial resolution of 0.94 × 0.94 × 1.0 mm^3 with a reconstruction matrix of 256 × 256, total scan duration: 7.5 min. The structural images were evaluated by an experienced neuroradiologist for further inspection in case of suspected brain anomalies.

2.4. Functional magnetic resonance imaging data preprocessing and analysis

The fMRI data were analyzed using two complementary approaches (Kriegeskorte and Bandettini, 2007b). Classical univariate analysis detects brain regions that exhibit higher or lower activity in Takotsubo patients compared to control subjects (Friston et al., 1994). This analysis reveals whether the subjects in a group, on average, have increased or decreased neural activity relative to the other group in a specific brain region when, for example, they are shown a particular emotional picture (Gilron et al., 2017). However, neural activity patterns are often highly individualized and heterogeneous across subjects (Kriegeskorte and Bandettini, 2007a). Furthermore, by averaging the neural activity of single voxels across, for example, a region of interest (ROI), some activity might go undetected. Thus, we also used multivariate pattern analysis (MVPA) to decode neural information that is discriminable for a certain experimental condition at the single-voxel-level. Thus, it is highly sensitive to fine-grained individual activity patterns (Haynes, 2015).

2.4.1. Univariate analysis

2.4.1.1. Preprocessing. As part of the univariate analysis, functional and structural MRI data were preprocessed with SPM12, revision 6906 (http://www.fil.ion.ucl.ac.uk/spm/software/spm12/) in MATLAB R2016a (https://ch.mathworks.com/products/matlab.html). The following preprocessing steps were successively performed using default SPM12 settings unless otherwise stated: (1) Slice time correction of the functional images; (2) Motion correction of the functional images by a rigid body transformation using six parameters (three translations and three rotations) in which the images were registered and then resliced to match the orientation of the first image; (3) Co-registration of the structural image to the mean functional image; (4) Segmentation and bias field correction of the structural image and estimation of deformation field parameters for spatial normalization to the T1-weighted MNI152 template; (5) Application of the deformation field parameters to the functional and structural images and subsequent reslicing of the functional images to an isotropic voxel size of 2 mm and reslicing of the structural images to an isotropic voxel size of 1 mm; and (6) Smoothing of the functional images with an 8 mm full width at half maximum (FWHM) three-dimensional Gaussian kernel.

2.4.1.2. First-level analysis. First-level analysis in SPM12 was based on a general linear model (GLM) of the voxel-wise BOLD signal time series for each subject (Friston et al., 1994). Separate models were specified and estimated for the expectation period and for the picture presentation period to avoid multicollinearity between regressors for the expectation and the respective picture (e.g., positive expectation and positive expected picture). In the "expectation model" design matrix, four regressors were defined for negative expectation (NegExp), positive expectation (PosExp), neutral expectation (NeutrExp), and unknown expectation (UnkExp). Each predictor was modeled as a boxcar function convolved with the canonical double-gamma hemodynamic response function (HRF), which lasted from the appearance of a cue to the end of the expectation period (duration: 7,920 ms). A high-pass filter of 128 s and the six motion parameters estimated during preprocessing were specified as nuisance regressors. The following contrasts of interest were computed for each subject: NegExp versus PosExp, NegExp versus NeutrExp, and PosExp versus NeutrExp.

In the "picture model" design matrix, five regressors were defined for negative expected pictures (NegExpPic), positive expected pictures (PosExpPic), neutral expected pictures (NeutrExpPic), negative unexpected pictures (NegUnexpPic), and positive unexpected pictures (PosUnexpPic). The regressors were again modelled as a boxcar function convolved with the canonical HRF from the start to the end of the picture presentation (duration: 7,920 ms). The nuisance regressors included a high-pass filter of 128 s and six motion parameters. The following contrasts were computed for each subject: NegExpPic versus PosExpPic, NegExpPic versus NeutrExpPic, PosExpPic versus NeutrExpPic, and NegUnexpPic versus PosUnexpPic.

2.4.1.3. . Second-level analysis. Between-subject random effects analysis was performed using non-parametric permutation tests implemented in the SPM toolbox SnPM13 (http://warwick.ac.uk/snpm). Permutation tests depend on fewer assumptions than standard parametric approaches and provide exact control of false positive rates (Eklund et al., 2016; Nichols and Holmes, 2002). The first-level contrast maps were entered as inputs for two-sample *t*-tests to compare Takotsubo patients and control subjects. The number of permutations was set to 10,000. Cluster inference on the cluster size was used with a cluster defining threshold (CDT) of $P = 0.001$ in conjunction with a neighborhood size of 26. The significance level was set to $P \leq 0.05$ family-wise error (FWE) corrected.

Two second-level masks were created a priori. The first mask restricted the analysis to voxels that were associated with the task-related terms "visual" and "emotional." The second mask restricted the analysis to gray-matter voxels and, therefore, excluded non-brain voxels, cerebrospinal fluid (CSF) voxels, and white-matter voxels. To create the visual-emotional mask, two separate reverse inference maps were downloaded from the automated meta-analysis tool Neurosynth (www.neurosynth.org) using the terms "visual" and "emotional." Reverse inference maps contain z-scores representing the likelihood that a particular term is used in a paper describing an fMRI study, given an activity in a particular brain region (Yarkoni et al., 2011). For the generation of the map associated with the term "visual", 2,549 studies were included. The map associated with the term "emotional" was based on 1,340 studies. These two z-score maps were then thresholded at $z = 3.1$, smoothed with a Gaussian kernel of 8 mm FWHM, binarized, and finally combined to form a single binary mask (see Supplementary Fig. 1). The gray-matter mask consisted of all 45 anatomical regions of the AAL atlas (Tzourio-Mazoyer et al., 2002), which were combined in a single map and subsequently binarized.

2.4.2. Multivariate pattern analysis

2.4.2.1. Preprocessing. The preprocessing of the functional and structural images for the MVPA differed from the preprocessing for the univariate analysis in two ways. First, during spatial normalization, the functional images were resliced to an isotropic voxel size of 3 mm. This modification had the advantage of reducing computation time. Second, in order to preserve the fine-grained patterns of activity, the functional images were not smoothed. These patterns may contain information about the experimental conditions (Kriegeskorte and Bandettini, 2007a).

2.4.2.2. First-level analysis. The MVPA first-level analysis was divided into two parts. First, parameter estimate images (beta images in SPM parlance) were extracted by modeling the voxel-wise BOLD signal time

series using a GLM (Mumford et al., 2012). A beta image contains voxel-wise regression weights for a particular regressor. Second, these beta images were decoded using searchlight analysis (Kriegeskorte et al., 2006). To extract the beta images, a separate GLM was specified and estimated for each contrast of interest. This step was different from the univariate first-level analysis, in which only two GLMs were specified and estimated (the "expectation model" and the "picture model"). The tested contrasts were identical to those in the univariate analysis. The design matrix for all the GLMs contained separate regressors for each event in the picture processing task. For example, in the "PosExp versus NegExp model", 14 regressors were defined for each of the positive expectation periods and 14 regressors were defined for each of the negative expectation periods. In addition, a high-pass filter of 128 s and six motion parameters were included as nuisance regressors. This procedure was repeated for all the contrasts of interest.

The resulting beta images were used as the input for the subsequent searchlight analysis. The searchlight analysis had the goal of decoding the experimental conditions within each contrast of interest from local activity patterns (e.g., decoding of PosExpPic versus NegExpPic). Therefore, the beta images were randomly divided into seven independent chunks for each contrast, with the restriction that each chunk contained an equal number of images per condition (e.g., two beta images from the PosExp condition and two beta images from the NegExp condition). Independence of the chunks was assumed for two reasons. First, the beta images were controlled for temporal autocorrelations by using a high-pass filter and they were also controlled for subject motion by including the motion parameters in the design matrix. Second, the events corresponding to single regressors in the design matrix were separated by more than 20 s. After this time window, the BOLD signal had returned to baseline (Etzel et al., 2011).

The searchlight analysis was conducted using the toolbox PyMVPA 2.6.1 (http://www.pymvpa.org/) in Python 2.7.13 (https://www.python.org/). Searchlight analysis (also known as information-based brain mapping) builds a map of voxels that are informative about the experimental conditions. Local activity patterns from multiple voxels can be used in combination with machine learning techniques to differentiate between experimental conditions. For example, a classifier decodes activity patterns about whether a subject was perceiving a positive expected picture or a negative expected picture at that time in the scanner. Brain regions that contain clusters of informative voxels are expected to be involved in the execution of the particular task at hand (Kriegeskorte and Bandettini, 2007a; Kriegeskorte et al., 2006).

One information map per contrast was created by moving a sphere across all the voxels. Each sphere had a radius of 9 mm and consisted of at most 122 surrounding voxels and one center voxel (see Fig. 1). In every sphere, a linear support vector machine was trained and tested using a 7-fold cross-validation that partitioned the aforementioned chunks. The average accuracy of the seven folds was then written into the center voxel of the sphere. The resulting information maps per subject and per contrast were subsequently smoothed with a Gaussian kernel of 8 mm FWHM before being subjected to second-level random effects analysis.

2.4.2.3. . Second-level analysis. Between-subject random effects analysis of the information maps was performed using non-parametric permutation tests as implemented in SnPM. Information maps for the Takotsubo patients and control subjects were compared using two-sample *t*-tests with the same settings as the univariate second-level analysis. Both the visual-emotional mask and the gray-matter mask were used to restrict the search space of the analysis. The group comparison of the information maps tested whether there were clusters of voxels in which the decoding of the experimental conditions was significantly higher or lower in the Takotsubo patients compared to the control subjects.

Differences in decoding between the two groups are unlikely to be relevant when the decoding of both groups is below the chance level (i.e. 50%). Therefore, it is necessary to test, within each group, whether it is possible to decode the conditions significantly above chance. Hence, regions of interest (ROIs) were created based on the significant clusters ($P \leq 0.05$ FWE-corrected) revealed by the group comparisons of the information maps. These ROIs were used for additional post-hoc decoding analyses. In this context, the experimental conditions were decoded again for all contrasts that revealed significant clusters. In contrast to the searchlight analysis, the pattern of the entire ROI was used as the input for decoding. In cases in which one contrast revealed multiple significant clusters, multiple ROIs were created and decoding was performed separately for each ROI (Etzel et al., 2013). Repeating this procedure for all the subjects resulted in one accuracy value per subject and ROI. These accuracies were analyzed separately for each group using the non-parametric one-sample Wilcoxon signed-rank test against chance level. The significance level was set to $P \leq 0.05$ (one-sided, Bonferroni-Holm corrected for multiple comparisons). The Wilcoxon signed-rank tests were performed using *R* (version 3.3.2, https://www.R-project.org/).

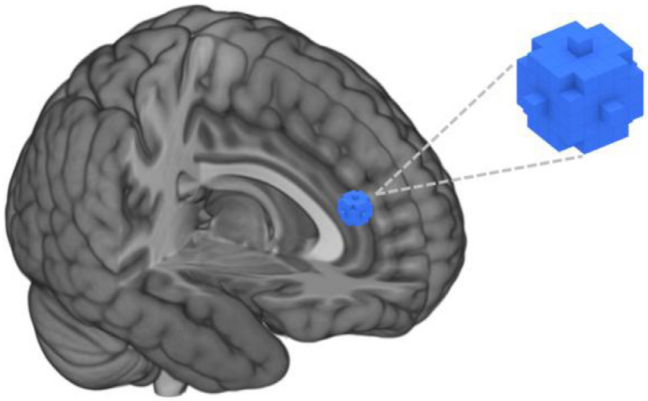

Fig. 1. Searchlight analysis. As an application of multivariate pattern analysis, searchlight analysis builds a map of voxels that are informative about the experimental conditions. A searchlight sphere (in blue) is moved across all the voxels of the brain. In every sphere, a linear support vector machine decodes the experimental conditions using an N-fold cross-validation approach. The average accuracy of the cross-validation fold is written in the center voxel of the searchlight sphere.

3. Results

3.1. Clinical characteristics

Takotsubo patients had significantly higher HADS anxiety scores than the control subjects ($t(45) = 2.70$, $P = 0.01$), but the two groups did not differ in their HADS depression scores ($t(45) = 1.75$, $P = 0.09$). Details about the clinical and demographical data as well as descriptive statistics are given in Table 1.

3.2. Results of the imaging data

As mentioned above, we analyzed fMRI data with two complementary analytical approaches. The first compared average differences between Takotsubo patients and matched control- subjects using classical univariate analysis. The second approach used MVPA (information-based analysis approach), which is based on the assumption that a neural activity *pattern* is different, and thus, discriminable between different experimental conditions. Hence, if information about a condition is present in the neural activity, this activity can be decoded; the more informative the activity pattern is, the better it can be decoded.

Table 1.
Demographical and clinical characteristics. Plus-minus values represent group means ± standard deviations. *P* values are given for two-tailed independent samples *t*-tests. Values of the left ventricular ejection fraction were obtained either during catheterization or echocardiography. If both were available, the values of the catheterization are reported.

Characteristic	Takotsubo patients (n = 26)	Control (n = 22)	*P* value
Age (years)	60 ± 15.54	55.36 ± 15.77	0.32
Female sex (no., %)	21 (81)	18 (82)	
Handedness (no., right / left)	25/1	22/0	
Time between Takotsubo syndrome episode and MRI (days)	822.42 ± 817.63		
MMSE (max. score = 30)	28.69 ± 1.93 (n = 26)	29.50 ± 0.67 (n = 22)	0.07
HADS anxiety (max. score = 21)	6.32 ± 4.09 (n = 25)	3.27 ± 3.58 (n = 22)	0.01
HADS depression (max. score = 21)	3.44 ± 3.69 (n = 25)	1.82 ± 2.44 (n = 22)	0.09
Chest pain (no., %, n = 25)	19 (76)		
Dyspnea (no., %, n = 25)	16 (64)		
High-sensitivity troponin T (ng/mL, n = 16) *	0.34 ± 0.17		
Creatine kinase (IU/L, n = 26) *	371.42 ± 632.70		
NT-proBNP (pg/mL, n = 17) *	5105.29 ± 9547.67		
ST-segment changes (no., %, n = 21)	3 (14)		
Heart rate (beats/minute, n = 22)	75.14 ± 14.76		
Systolic blood pressure (mmHg, n = 24)	120.71 ± 29.78		
Left ventricular ejection fraction (%, n = 26)	45.46 ± 13.91		
Left ventricular end diastolic pressure (mmHg, n = 22)	21.77 ± 4.31		
Coronary artery disease (no., %, n = 24)	4 (17)		
Recurrence of Takotsubo syndrome (no., %)	3 (12)		

Abbreviations: HADS, Hospital Anxiety and Depression Scale; max, maximum; MMSE, Mini-Mental State Examination; n, number of subjects; NT-proBNP, N-terminal prohormone of brain natriuretic peptide.
*value upon hospital admission

3.2.1. Results of the classical univariate analysis

The second-level univariate analysis with the visual-emotional mask revealed the following significant differences in activity. The Takotsubo patients showed significantly lower mean activity than the control subjects in the left (P = 0.048) and right superior parietal lobe (P = 0.043) during the processing of negative expected pictures in comparison to positive expected pictures. The significant clusters are shown in Fig. 2A. Detailed statistics and the coordinates of the significant clusters are given in Table 2. No other contrasts of interest analyzed with the visual-emotional mask were found to have significant group differences in activity in the univariate analysis. The univariate group comparison with the gray-matter mask found no significant differences in activity for any of the contrasts of interest. All reported *P*-values were FWE-corrected for multiple comparisons at cluster level.

3.2.2. Results of the multivariate pattern analysis

The second-level MVPA with the visual-emotional mask revealed significant differences in decoding accuracy between Takotsubo patients and control subjects: As shown in Fig. 2B, Takotsubo patients showed significantly lower decoding of negative expectation versus positive expectation in the right intracalcarine cortex (P = 0.001) and the left lingual gyrus (P = 0.007). As shown in Fig. 2C, Takotsubo patients also showed significantly lower decoding of negative expected pictures versus neutral expected pictures in the left lateral occipital cortex (P = 0.005), the right middle frontal gyrus (P = 0.014), and the right temporo-occipital fusiform cortex (P = 0.017). No further contrasts of interest of the second-level MVPA with the visual-emotional mask revealed differences in decoding accuracy between the two groups. Detailed statistics and the coordinates of the significant clusters are given in Table 3.

The second-level MVPA with the gray-matter mask revealed similar differences in decoding accuracy between the Takotsubo patients and control subjects. As shown in Fig. 2B, Takotsubo patients showed significantly lower decoding of negative expectation versus positive expectation in the right intracalcarine cortex (P = 0.009) and the left lingual gyrus (P = 0.034). As shown in Fig. 2C, Takotsubo patients showed significantly lower decoding of negative expected pictures versus neutral expected pictures in the left supramarginal gyrus (P = 0.004), the right superior frontal gyrus (P = 0.012), the superior part of the left lateral occipital cortex (P = 0.021), the pars opercularis of the left inferior frontal gyrus (P = 0.026), the posterior part of the left supramarginal gyrus (P = 0.027), the posterior part of the right supramarginal gyrus (P = 0.027), and the left cerebellar vermis VI (P = 0.047). Detailed statistics and the coordinates of the significant clusters are given in Table 4. All reported *P* values are FWE-corrected for multiple comparisons at cluster level.

3.2.3. Post-hoc regions of interest decoding

Post-hoc ROI decoding confirmed the results of the MVPA searchlight analysis (see Supplementary Figs. 2 and 3). Takotsubo patients showed chance-level decoding of negative expectation versus positive expectation, and negative expected pictures versus neutral expected pictures in all the ROIs we investigated (Bonferroni-Holm corrected $P > 0.05$). In contrast, control subjects showed decoding above chance-level in all the ROIs that were investigated (Bonferroni–Holm corrected $P < 0.05$), except the right intracalcarine cortex, as defined by the MVPA second-level analysis, using the visual-emotional mask (Bonferroni–Holm corrected P = 0.06). The statistical details are given in Supplementary Tables 1 and 2.

4. Discussion

The present study demonstrates neural differences between Takotsubo patients and control subjects during an emotional picture processing task using two complementary analytical approaches. First, classical univariate analysis was used to reveal brain regions that showed differences in mean activity between the two groups. This analysis found that Takotsubo patients exhibited lower activity than control subjects in the bilateral superior parietal lobe when processing negative expected pictures than when processing positive expected pictures. Second, individual activity patterns were decoded using MVPA, which revealed that Takotsubo patients showed lower decoding of negative expected pictures versus neutral expected pictures in regions in the frontal cortex (the right superior frontal gyrus, right middle frontal gyrus, and left inferior frontal gyrus), parietal cortex (the bilateral supramarginal gyrus), visual cortex (the left lateral occipital cortex and right temporal occipital fusiform cortex), and the cerebellum (the left vermis VI). Takotsubo patients also exhibited lower decoding of negative expectation versus positive expectation in the visual cortex (the right intracalcarine cortex and left lingual gyrus) and had a higher

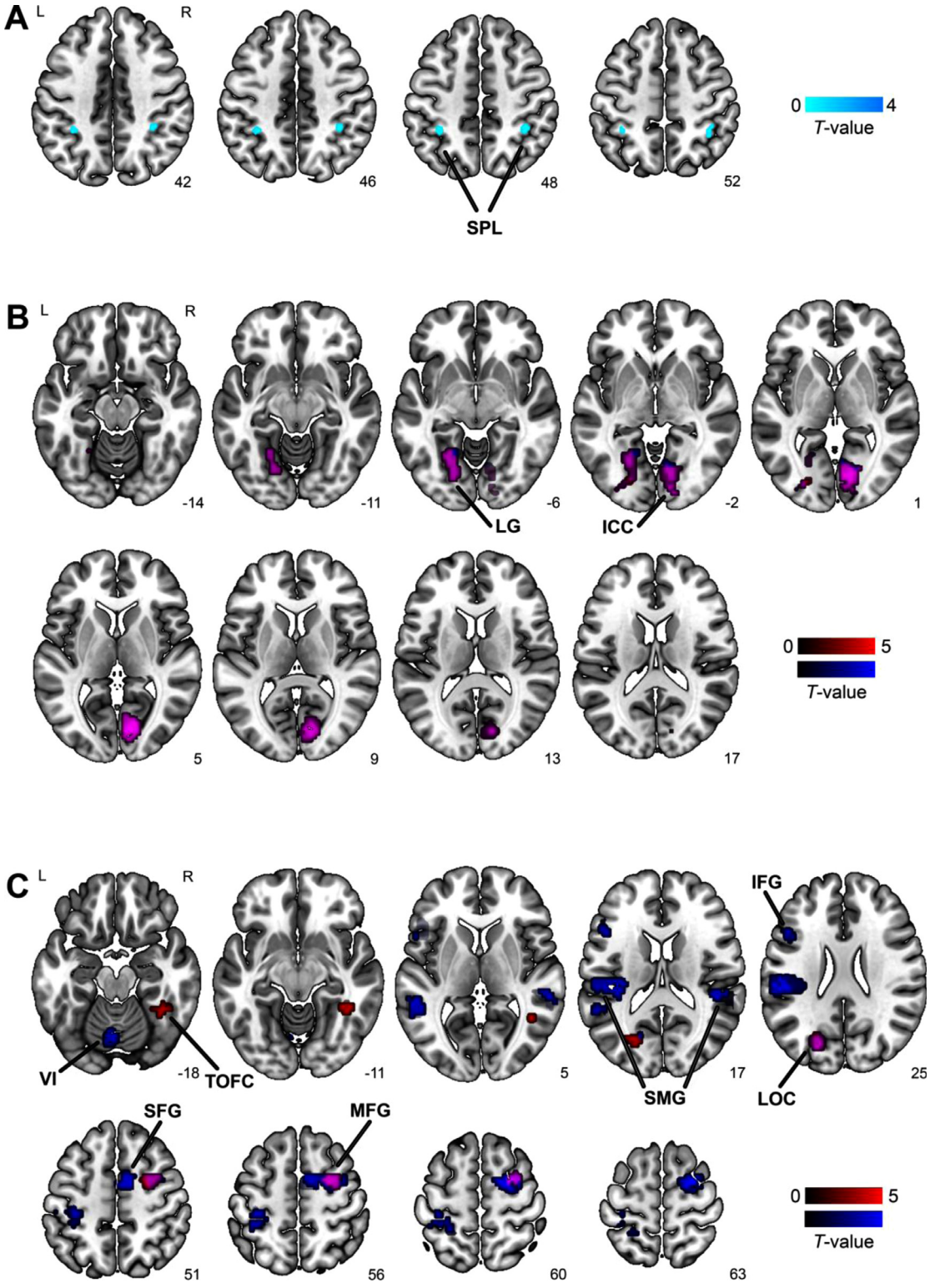

Fig. 2. Second-level results of the univariate analysis and the multivariate pattern analysis. A) Takotsubo patients showed lower activity in the bilateral superior parietal lobe (SPL) in response to negative expected pictures compared to positive expected pictures. Significant clusters in the univariate analysis, using the visual-emotional mask, are shown in cyan. B) Takotsubo patients showed lower decoding of negative expectation versus positive expectation in the right intracalcarine cortex (ICC) and the left lingual gyrus (LG). Significant clusters in the multivariate pattern analysis, using the visual-emotional mask, are shown in red. Significant clusters in the multivariate pattern analysis, using the gray-matter mask, are shown in blue. The overlap of the clusters of the analyses with the two masks are shown in pink. C) Takotsubo patients showed significantly lower decoding of negative expected pictures versus neutral expected pictures in the bilateral supramarginal gyrus (SMG), the right superior frontal gyrus (SFG), the right middle frontal gyrus (MFG), the left inferior frontal gyrus (IFG), the right temporal occipital fusiform cortex (TOFC), the left lateral occipital cortex (LOC), and the left cerebellar vermis (VI). Significant clusters of the multivariate pattern analysis, using the visual-emotional mask are shown in red, and significant clusters of the multivariate pattern analysis, using the gray-matter mask, are shown in blue. The overlap of the clusters of the analyses with the two-masks are shown in pink. All clusters are significant at $P \leq 0.05$, family-wise error corrected.

Table 2.
Results of the univariate analysis. Second-level summary statistics of the univariate analysis with the visual-emotional mask, given for each significant contrast and cluster separately ($P \leq 0.05$, family-wise error corrected, minimum cluster size $k = 10$). Probability of brain regions (in %) given according to the Harvard-Oxford cortical atlas (https://fsl.fmrib.ox.ac.uk/fsl/fslwiki/Atlases).

Group contrast	Condition contrast	Number of voxels	Max. *t* value	MNI coordinates max. *t* value (*x*, *y*, *z*)	MNI coordinates center of gravity (*x*, *y*, *z*)	Brain regions' center of gravity	*P* value
Control subjects > Takotsubo patients	NegExpPic > PosExpPic	76	3.88	36, −42, 46	36.5, −43.7, 48.3	50% R superior parietal lobe 7% R supramarginal gyrus (post.)	0.043
		69	3.88	−34, −46, 46	−33.5, −44.5, 45.6	33% L superior parietal lobe 12% L supramarginal gyrus (post.)	0.048

Abbreviations: L, left; Max, maximal; MNI, Montreal Neurological Institute; NegExpPic, negative expected picture; PosExpPic, positive expected picture; post, posterior; R, right.

level of anxiety but not depression, according to the HADS, compared to the healthy control group.

The superior parietal lobe is part of the fronto-parietal central executive network (Seeley et al., 2007), which consists of brain regions that play an important role in the regulation of emotions (Etkin et al., 2015). Emotion regulation can be broadly defined as a set of processes intended to modulate the trajectory of an emotion (Gross, 2015). Individuals often downregulate upcoming negative emotions by using emotional regulation strategies, such as cognitive reappraisal, which is the explicit re-evaluation of an emotional stimulus to reduce its emotional relevance. Meta-analyses of neuroimaging studies on cognitive reappraisal consistently show increased activity in the superior parietal lobe, among others, as part of the fronto-parietal central executive network (Kohn et al., 2014).

The present study found lower activity in the bilateral superior parietal lobe of Takotsubo patients compared to the controls in response to negative expected pictures. However, we did not observe group differences in activity in response to negative unexpected pictures. Given the crucial role of the parietal lobe in emotion regulation, these findings may reflect impaired regulation of emotions in the Takotsubo patients. Subjects had the opportunity to use emotion-regulation strategies for negative expected pictures, as the appearance of the pictures was signaled by a cue that allowed subjects to prepare for the subsequent picture. Although using emotion-regulation strategies was more difficult for unexpected pictures because no cue was presented before the picture, it seems as if Takotsubo patients used inappropriate or no emotion regulation at all, even in the case of the expected pictures. Impaired emotion regulation in Takotsubo patients has been observed in behavioral studies (Compare et al., 2013; Hefner and Csef, 2013; Sabisz et al., 2016). For example, the results of a study that used self-report measures of stress management and personality traits that are associated with inappropriate emotion-regulation strategies indicated that patients were less likely to use beneficial emotional regulation strategies, such as the cognitive reappraisal strategy of de-emphasizing (Hefner and Csef, 2013). In addition, an association between Takotsubo syndrome and Type D personality was found (Compare et al., 2013), which is frequently observed in patients with depression or anxiety (Denollet and Kupper, 2007; Spindler et al., 2007). These findings are in line with the increased anxiety observed in our Takotsubo patients as well as the proposed association between Takotsubo syndrome and psychiatric symptoms (Templin et al., 2015).

A further explanation for the reduced activity of the superior parietal lobe in the patient group involves its role in the central control of the sympathetic nervous system (Beissner et al., 2013). As mentioned above, many brain regions involved in the central control of the autonomic nervous system are also involved in processing and regulating emotions (Beissner et al., 2013; Etkin et al., 2015; Lindquist et al., 2012) and have been shown to be altered in Takotsubo syndrome (Hiestand et al., 2018; Klein et al., 2017; Pereira et al., 2016; Sabisz et al., 2016; Suzuki et al., 2014). Thus, as the activity of the autonomic nervous system can be considered a physiological component of emotional processing (Kreibig, 2010), the lower activity in the superior parietal lobe might reflect a complex relationship between emotions and the autonomic nervous system in Takotsubo patients.

The MVPA found group differences in decoding of negative expected pictures versus neutral expected pictures. In the control subjects, these conditions could be decoded from the activity patterns of a widespread network that included the frontal and parietal lobes, the visual cortex, and the cerebellum. However, as shown by the chance-level decoding, the processing of both types of images was similar in the Takotsubo patients, which indicates comparable neural activity when processing pictures with different valences (Kriegeskorte et al., 2006).

The dorsolateral prefrontal cortex (the superior and middle frontal gyrus), the ventrolateral prefrontal cortex (inferior frontal gyrus), and the parietal cortex (supramarginal gyrus) are part of the fronto-parietal central executive network, and are therefore strongly involved in the

Table 3.
Results of the visual-emotional mask-based multivariate pattern analysis. Second-level summary statistics of the multivariate pattern analysis with the visual-emotional mask, given for each significant contrast and cluster separately ($P \leq 0.05$, family-wise error corrected, minimum cluster size $k = 10$). Probability of brain regions (in %) given according to the Harvard-Oxford cortical atlas (https://fsl.fmrib.ox.ac.uk/fsl/fslwiki/Atlases).

Group contrast	Condition contrast	Number of voxels	Max. *t* value	MNI coordinates max. *t* value (*x, y, z*)	MNI coordinates center of gravity (*x, y, z*)	Brain regions' center of gravity	*P* value
Control subjects > Takotsubo patients	NegExp versus PosExp	161	5.06	12, −79, 5	11.9, −78, 3.88	47% R intracalcarine cortex 18% R lingual gyrus	0.001
		84	3.81	−18, −76, −7	−21.6, −68, −5.39	31% L lingual gyrus 19% L occipital fusiform gyrus	0.007
Control subjects > Takotsubo patients	NegExpPic versus NeutrExpPic	148	4.1	−24, −76, 41	−22.2, −74.6, 31	21% L lateral occipital cortex 5% L cuneal cortex	0.005
		69	4.88	24, −4, 59	28.2, −1.28, 53.2	26% R middle frontal gyrus 18% R superior frontal gyrus	0.014
		61	3.94	42, −52, 5	40.5, −47.5, −9.94	8% R temporal occipital fusiform cortex 6% R inferior temporal gyrus (temporooccipital part)	0.017

Abbreviations: L, left; Max, maximal; MNI, Montreal Neurological Institute; NegExp, negative expectation; NegExpPic, negative expected picture; NeutrExpPic, neutral expected picture; PosExp, positive expectation; post, posterior; R, right.

regulation of emotions (Etkin et al., 2015; Seeley et al., 2007). Intriguingly, the cerebellum is also associated with the central executive network (Habas et al., 2009), but its exact role in emotion regulation is still unclear (Adamaszek et al., 2017). No regulation of emotions is required when neutral pictures are presented, in contrast to the processing of negative pictures. This is putatively reflected in the differential activity patterns of the control subjects in these two conditions. Hence, the similar pattern of activity observed in the Takotsubo patients during the processing of negative and neutral expected pictures may be indicative of impaired emotion regulation.

According to a meta-analysis of the processing of emotional pictures in healthy subjects, visual cortex activity is consistently higher in response to emotional pictures than in response to neutral pictures (Sabatinelli et al., 2011). This finding is consistent with the above-chance decoding of negative versus neutral expected pictures in the visual cortex of the control subjects in our study. It has been suggested that differential activity during the processing of emotional and neutral stimuli is influenced by attentional processes that facilitate more elaborate processing of emotional stimuli (Bradley et al., 2003). Following this line of argumentation, the Takotsubo-specific similarity in the activity patterns in response to positive and negative pictures might indicate a less elaborated processing of the negative pictures.

Negative expectation versus positive expectation was decoded in the control subjects from the bilateral visual cortex activity patterns. Previous studies of healthy subjects have shown differential activity patterns in the visual cortex during the expectation of negative versus positive visual stimuli (Herwig et al., 2007a,b). In contrast, the visual cortex activity patterns of the Takotsubo patients did not contain information about these experimental conditions. This suggests that the patterns of visual cortex activity of the control subjects during the two expectation periods (positive and negative) were distinct, whereas the activity patterns of the Takotsubo patients were too similar to be differentiated (Kriegeskorte et al., 2006). As previously mentioned, there might be a Takotsubo-specific impairment in the regulation of emotions during the processing of negative expected pictures, presumably because Takotsubo patients do not appropriately prepare for the appearance of the pictures. In the framework of predictive coding, the activity patterns might reflect predictions about future stimuli. All sensory systems (e.g., the visual system or the auditory system) constantly make predictions about upcoming sensory stimuli. These predictions are subsequently compared with the actual stimuli encountered. If there is a mismatch between the predicted and the actual stimuli, a prediction error is generated, and future predictions are modified (Rao and Ballard, 1999). This is relevant to our results as the visual cortex plays an important role in forming and modifying these predictions of visual stimuli (den Ouden et al., 2009; Kok et al., 2014). Of note, it has been demonstrated that the nature of an upcoming stimulus can be accurately decoded during the expectation of that stimulus (Kok et al., 2017). Interestingly, recent studies have found impaired predictive coding in patients with anxiety (Etkin and Fonzo, 2017; White et al., 2017) as well as anxious healthy subjects (Cornwell et al., 2017). It has been suggested that patients with anxiety have an impaired ability to modify predictions following prediction errors (White et al., 2017). The results of the present study thus suggest that Takotsubo patients perform inadequate predictions during the expectation of an emotional stimulus. However, given the experimental paradigm used in our study, we cannot determine whether these inadequate predictions are a result of impaired prediction errors or another undetermined process.

5. Limitations and outlook

In the following, we want to address some limitations, which could be addressed in future investigations on the same topic. First, the passive task used in this study had a slow event-related design because we wanted to avoid emotional exhaustion of the patients caused by a high number of stimuli in close succession. If feasible, future studies might use a block or a fast event-related task design to increase the number of trials and thus the statistical power to detect subtle differences between the groups. Second, somewhat surprisingly, we did not find group differences in the amygdala activity, neither with the univariate nor the multivariate analysis approaches. As the amygdala is a relatively small structure, the voxel-based analyses we used might not be sensitive enough to detect subtle group differences in this brain region. Thus, future studies might apply a more sensitive ROI-based approach to increase the sensitivity for potential group differences in amygdala activity.

6. Conclusion

The present study is the first to investigate the neural correlates of emotional regulation and processing in Takotsubo patients using fMRI. The results of the study suggest that there are Takotsubo-specific deficits in emotion regulation and processing that may be related to deficits in predictive coding. This deficient regulation of emotions might play a further factor in the origins of this brain-heart disease, but further studies are necessary for a deeper and more profound understanding of its exact role.

Data sharing statement

Due to sensitive nature of the patients enrolled in the study, subjects

Table. 4
Results of the gray-matter mask-based multivariate pattern analysis. Second-level summary statistics of the multivariate pattern analysis with the gray-matter mask, given for each significant contrast and cluster separately ($P \leq 0.05$, family-wise error corrected, minimum cluster size $k = 10$). Probability of brain regions (in %) given according to the Harvard-Oxford cortical atlas (https://fsl.fmrib.ox.ac.uk/fsl/fslwiki/Atlases).

Group contrast	Condition contrast	Number of voxels	Max. *t* value	MNI coordinates max. *t* value (*x*, *y*, *z*)	MNI coordinates center of gravity (*x*, *y*, *z*)	Brain regions' center of gravity	*P* value
Control subjects > Takotsubo patients	NegExp versus PosExp	169	5.06	12, −79, 5	11.9, −77.5, 3.67	47% R intracalcarine cortex 18% R lingual gyrus	0.009
		88	3.81	−18, −76, −7	−21.2, −66.7, −5.49	37% L lingual gyrus 14% L occipital fusiform gyrus	0.034
Control subjects > Takotsubo patients	NegExpPic versus NeutrExpPic	365	4.81	−60, −28, 29	−46.2, −27.6, 31.8	16% L supramarginal gyrus 4% L postcentral gyrus	0.004
		198	5.13	27, −4, 65	20.6, −2.35, 56.2	44% R superior frontal gyrus 9% R precentral gyrus	0.012
		128	4.10	−24, −78, 41	−21.9, −75, 33	26% L lateral occipital cortex (sup.) 4% L cuneal cortex	0.021
		109	3.98	−51, 26, 11	−46.4, 16.1, 18.1	39% L inferior frontal gyrus (pars opercularis) 3% L inferior frontal gyrus (pars triangularis)	0.026
		106	4.15	−57, −40, 2	−53.3, −44.6, 8.89	34% L supramarginal gyrus (post.) 12% L middle temporal gyrus	0.027
		105	4.22	54, −34, 11	53.2, −36.1, 11.9	17% R supramarginal gyrus (post.) 7% R superior temporal gyrus (post.)	0.027
		68	3.91	−6, −70, −22	−4.25, −70.2, −20.9	67% L vermis VI 27% L VI	0.047

Abbreviations: L, left; Max, maximal; MNI, Montreal Neurological Institute; NegExp, negative expectation; NegExpPic, negative expected picture; NeutrExpPic, neutral expected picture; PosExp, positive expectation; post, posterior; R, right.

were assured that data would remain confidential and would not be shared.

Funding

This project was supported by the Foundation for Cardiovascular Research – Zurich Heart House, by research grants from the Swiss Heart Foundation, and the H.H. Sheikh Khalifa bin Hamad Al-Thani Research Program to CT, and by the University Research Priority Program "Dynamics of Healthy Aging" to LJ.

CRediT authorship contribution statement

Carina Klein: Conceptualization, Data curation, Formal analysis, Investigation, Software, Project administration, Writing - original draft. **Simon Leipold:** Formal analysis, Investigation, Methodology, Software, Writing - original draft. **Jelena-Rima Ghadri:** Conceptualization, Project administration, Resources, Supervision, Validation, Writing - original draft. **Stjepan Jurisic:** Writing - review & editing, Resources, Project administration. **Thierry Hiestand:** Resources, Writing - review & editing, Project administration. **Jürgen Hänggi:** Project administration, Writing - review & editing, Software, Formal analysis. **Thomas F. Lüscher:** Conceptualization, Project administration, Resources, Writing - review & editing. **Lutz Jäncke:** Conceptualization, Funding acquisition, Methodology, Project administration, Resources, Supervision, Validation, Writing - review & editing. **Christian Templin:** Conceptualization, Funding acquisition, Project administration, Resources, Supervision, Validation, Writing - review & editing.

Declaration of Competing Interest

None.

Acknowledgements

We thank all the Takotsubo patients and healthy subjects for participation in our study.

Supplementary materials

Supplementary material associated with this article can be found, in the online version, at doi:10.1016/j.nicl.2019.102124.

References

Adamaszek, M., D'Agata, F., Ferrucci, R., Habas, C., Keulen, S., Kirkby, K.C., Leggio, M., Mariën, P., Molinari, M., Moulton, E., Orsi, L., Van Overwalle, F., Papadelis, C., Priori, A., Sacchetti, B., Schutter, D.J., Styliadis, C., Verhoeven, J., 2017. Consensus paper: cerebellum and emotion. Cerebellum 16, 552–576.

Annett, M., 1970. A classification of hand preference by association analysis. Br. J. Psychol. 61, 303–321.

Beissner, F., Meissner, K., Bär, K.-J., Napadow, V., 2013. The autonomic brain: an activation likelihood estimation meta-analysis for central processing of autonomic function. J. Neurosci. 33, 10503–10511.

Borchert, T., Hubscher, D., Guessoum, C.I., Lam, T.D., Ghadri, J.R., Schellinger, I.N., Tiburcy, M., Liaw, N.Y., Li, Y., Haas, J., Sossalla, S., Huber, M.A., Cyganek, L., Jacobshagen, C., Dressel, R., Raaz, U., Nikolaev, V.O., Guan, K., Thiele, H., Meder, B., Wollnik, B., Zimmermann, W.H., Luscher, T.F., Hasenfuss, G., Templin, C., Streckfuss-Bomeke, K., 2017. Catecholamine-dependent beta-adrenergic signaling in a pluripotent stem cell model of Takotsubo cardiomyopathy. J. Am. Coll. Cardiol. 70, 975–991.

Bradley, M.M., Sabatinelli, D., Lang, P.J., Fitzsimmons, J.R., King, W., Desai, P., 2003. Activation of the visual cortex in motivated attention. Behav. Neurosci. 117, 369–380.

Button, K.S., Ioannidis, J.P.A., Mokrysz, C., Nosek, B.A., Flint, J., Robinson, E.S.J., Munafo, M.R., 2013. Power failure: why small sample size undermines the reliability of neuroscience. Nat. Rev. Neurosci. 14, 365–376.

Compare, A., Bigi, R., Orrego, P.S., Proietti, R., Grossi, E., Steptoe, A., 2013. Type D personality is associated with the development of Stress Cardiomyopathy following emotional triggers. Ann. Behav. Med. 45, 299–307.

Cornwell, B.R., Garrido, M.I., Overstreet, C., Pine, D.S., Grillon, C., 2017. The unpredictive brain under threat: a neurocomputational account of anxious hypervigilance. Biol. Psychiatry 82, 447–454.

den Ouden, H.E.M., Friston, K.J., Daw, N.D., McIntosh, A.R., Stephan, K.E., 2009. A dual role for prediction error in associative learning. Cereb. Cortex 19, 1175–1185.

Denollet, J., Kupper, N., 2007. Type-D personality, depression, and cardiac prognosis: cortisol dysregulation as a mediating mechanism. J. Psychosom. Res. 62, 607–609.

Eklund, A., Nichols, T.E., Knutsson, H., 2016. Cluster failure: why fMRI inferences for spatial extent have inflated false-positive rates. Proc. Natl. Acad. Sci. USA 113, 7900–7905.

Etkin, A., Büchel, C., Gross, J.J., 2015. The neural bases of emotion regulation. Nat. Rev. Neurosci. 16, 693.

Etkin, A., Fonzo, G.A., 2017. Learning in Generalized Anxiety Disorder benefits from neither the carrot nor the stick. Am. J. Psychiatry 174, 87–88.

Etzel, J.A., Valchev, N., Keysers, C., 2011. The impact of certain methodological choices on multivariate analysis of fMRI data with support vector machines. NeuroImage 54, 1159–1167.

Etzel, J.A., Zacks, J.M., Braver, T.S., 2013. Searchlight analysis: promise, pitfalls, and potential. Neuroimage 78, 261–269.

Folstein, M.F., Folstein, S.E., McHugh, P.R., 1975. "Minimental-State": a practical method for grading the cognitive state of patients for the clinician. J. Psychiatr. Res. 12, 189–198.

Friston, K.J., Holmes, A.P., Worsley, K.J., Poline, J.P., Frith, C.D., Frackowiak, R.S.J., 1994. Statistical parametric maps in functional imaging: a general linear approach. Hum. Brain Mapp. 2, 189–210.

Ghadri, J.R., Sarcon, A., Diekmann, J., Bataiosu, D.R., Cammann, V.L., Jurisic, S., Napp, L.C., Jaguszewski, M., Scherff, F., Brugger, P., Jäncke, L., Seifert, B., Bax, J.J., Ruschitzka, F., Luscher, T.F., Templin, C., Inter, T.A.K.C., 2016. Happy heart syndrome: role of positive emotional stress in Takotsubo syndrome. Eur. Heart J. 37, 2823–2829.

Ghadri, J.R., Wittstein, I.S., Prasad, A., Sharkey, S., Dote, K., Akashi, Y.J., Cammann, V.L., Crea, F., Galiuto, L., Desmet, W., Yoshida, T., Manfredini, R., Eitel, I., Kosuge, M., Nef, H.M., Deshmukh, A., Lerman, A., Bossone, E., Citro, R., Ueyama, T., Corrado, D., Kurisu, S., Ruschitzka, F., Winchester, D., Lyon, A.R., Omerovic, E., Bax, J.J., Meimoun, P., Tarantini, G., Rihal, C., S, Y.H., Migliore, F., Horowitz, J.D., Shimokawa, H., Luscher, T.F., Templin, C., 2018a. International expert consensus document on Takotsubo Syndrome (Part I): clinical characteristics, diagnostic criteria, and pathophysiology. Eur. Heart J. 39, 2032–2046.

Ghadri, J.R., Wittstein, I.S., Prasad, A., Sharkey, S., Dote, K., Akashi, Y.J., Cammann, V.L., Crea, F., Galiuto, L., Desmet, W., Yoshida, T., Manfredini, R., Eitel, I., Kosuge, M., Nef, H.M., Deshmukh, A., Lerman, A., Bossone, E., Citro, R., Ueyama, T., Corrado, D., Kurisu, S., Ruschitzka, F., Winchester, D., Lyon, A.R., Omerovic, E., Bax, J.J., Meimoun, P., Tarantini, G., Rihal, C., S, Y.H., Migliore, F., Horowitz, J.D., Shimokawa, H., Luscher, T.F., Templin, C., 2018b. International expert consensus document on Takotsubo Syndrome (Part II): diagnostic workup, outcome, and management. Eur. Heart J. 39, 2047–2062.

Gilron, R., Rosenblatt, J., Koyejo, O., Poldrack, R.A., Mukamel, R., 2017. What's in a pattern? Examining the type of signal multivariate analysis uncovers at the group level. NeuroImage 146, 113–120.

Gross, J.J., 2015. Emotion regulation: current status and future prospects. Psychol. Inq. 26, 1–26.

Habas, C., Kamdar, N., Nguyen, D., Prater, K., Beckmann, C.F., Menon, V., Greicius, M.D., 2009. Distinct cerebellar contributions to intrinsic connectivity networks. J. Neurosci. 29, 8586.

Haynes, J.-D., 2015. A primer on pattern-based approaches to fMRI: principles, pitfalls, and perspectives. Neuron 87, 257–270.

Hefner, J., Csef, H., 2013. Unfavorable stress management strategies in patients with Tako-Tsubo Cardiomyopathy (TTC). Int. J. Cardiol. 168, 4582–4583.

Herwig, U., Baumgartner, T., Kaffenberger, T., Brühl, A., Kottlow, M., Schreiter-Gasser, U., Abler, B., Jäncke, L., Rufer, M., 2007a. Modulation of anticipatory emotion and perception processing by cognitive control. NeuroImage 37, 652–662.

Herwig, U., Kaffenberger, T., Baumgartner, T., Jäncke, L., 2007b. Neural correlates of a 'pessimistic' attitude when anticipating events of unknown emotional valence. NeuroImage 34, 848–858.

Hiestand, T., Hänggi, J., Klein, C., Topka, M.S., Jaguszewski, M., Ghadri, J.R., Lüscher, T.F., Jäncke, L., Templin, C., 2018. Takotsubo Syndrome associated with structural brain alterations of the limbic system. J. Am. Coll. Cardiol. 71, 809–811.

Jaguszewski, M., Osipova, J., Ghadri, J.R., Napp, L.C., Widera, C., Franke, J., Fijalkowski, M., Nowak, R., Fijalkowska, M., Volkmann, I., Katus, H.A., Wollert, K.C., Bauersachs, J., Erne, P., Luscher, T.F., Thum, T., Templin, C., 2014. A signature of circulating microRNAs differentiates Takotsubo cardiomyopathy from acute myocardial infarction. Eur. Heart J. 35, 999–1006.

Klein, C., Hiestand, T., Ghadri, J.-R., Templin, C., Jäncke, L., Hänggi, J., 2017. Takotsubo Syndrome – predictable from brain imaging data. Sci. Rep. 7.

Kohn, N., Eickhoff, S.B., Scheller, M., Laird, A.R., Fox, P.T., Habel, U., 2014. Neural network of cognitive emotion regulation – an ALE meta-analysis and MACM analysis. NeuroImage 87, 345–355.

Kok, P., Failing, M.F., de Lange, F.P., 2014. Prior expectations evoke stimulus templates in the primary visual cortex. J. Cognit. Neurosci. 26, 1546–1554.

Kok, P., Mostert, P., de Lange, F.P., 2017. Prior expectations induce prestimulus sensory templates. Proc. Natl. Acad. Sci. USA 114, 10473–10478.

Kreibig, S.D., 2010. Autonomic nervous system activity in emotion: a review. Biol. Psychiatry 84, 394–421.

Kriegeskorte, N., Bandettini, P.A., 2007a. Analyzing for information, not activation, to exploit high-resolution fMRI. NeuroImage 38, 649–662.

Kriegeskorte, N., Bandettini, P.A., 2007b. Combining the tools: activation- and information-based fMRI analysis. NeuroImage 38, 666–668.

Kriegeskorte, N., Goebel, R., Bandettini, P.A., 2006. Information-based functional brain

mapping. Proc. Natl. Acad. Sci. USA 103, 3863–3868.
Lang, P.J., Bradley, M.M., Cuthbert, B.N., 1995. International Affective Picture System (IAPS): technical manual and affective ratings. National Institute of Mental Health Center for the Study of Emotion and Attention. University of Florida, Gainesville, FL.
Lindquist, K.A., Wager, T.D., Kober, H., Bliss-Moreau, E., Barrett, L.F., 2012. The brain basis of emotion: a meta-analytic review. Behav. Brain Sci. 35, 121–143.
Mumford, J.A., Turner, B.O., Ashby, F.G., Poldrack, R.A., 2012. Deconvolving BOLD activation in event-related designs for multivoxel pattern classification analyses. NeuroImage 59, 2636–2643.
Napp, L.C., Ghadri, J.R., Bauersachs, J., Templin, C., 2015a. Acute coronary syndrome or Takotsubo cardiomyopathy: the suspect may not always be the culprit. Int. J. Cardiol. 187, 116–119.
Napp, L.C., Ghadri, J.R., Cammann, V.L., Bauersachs, J., Templin, C., 2015b. Takotsubo cardiomyopathy: completely simple but not so easy. Int. J. Cardiol. 197, 257–259.
Nichols, T.E., Holmes, A.P., 2002. Nonparametric permutation tests for functional neuroimaging: a primer with examples. Hum. Brain Mapp. 15, 1–25.
Pereira, V.H., Marques, P., Magalhaes, R., Portugues, J., Calvo, L., Cerqueira, J.J., Sousa, N., 2016. Central autonomic nervous system response to autonomic challenges is altered in patients with a previous episode of Takotsubo cardiomyopathy. Eur. Heart J. Acute Cardiovasc. Care 5, 152–163.
Rao, R.P.N., Ballard, D.H., 1999. Predictive coding in the visual cortex: a functional interpretation of some extra-classical receptive-field effects. Nat. Neurosci. 2, 79.
Sabatinelli, D., Fortune, E.E., Li, Q., Siddiqui, A., Krafft, C., Oliver, W.T., Beck, S., Jeffries, J., 2011. Emotional perception: meta-analyses of face and natural scene processing. NeuroImage 54, 2524–2533.
Sabisz, A., Treder, N., Fijalkowska, M., Sieminski, M., Fijalkowska, J., Naumczyk, P., Nowak, R., Jaguszewski, M., Cwalina, N., Gruchala, M., Szurowska, E., Fijalkowski, M., 2016. Brain resting state functional magnetic resonance imaging in patients with Takotsubo cardiomyopathy an inseparable pair of brain and heart. Int. J. Cardiol. 224, 376–381.
Seeley, W.W., Menon, V., Schatzberg, A.F., Keller, J., Glover, G.H., Kenna, H., Reiss, A.L., Greicius, M.D., 2007. Dissociable intrinsic connectivity networks for salience processing and executive control. J. Neurosci. 27, 2349.
Spindler, H., Pedersen, S.S., Serruys, P.W., Erdman, R.A.M., van Domburg, R.T., 2007. Type-D personality predicts chronic anxiety following percutaneous coronary intervention in the drug-eluting stent era. J. Affect. Disord. 99, 173–179.
Steptoe, A., Kivimaki, M., 2012. Stress and cardiovascular disease. Nat. Rev. Cardiol. 9, 360–370.
Suzuki, H., Matsumoto, Y., Kaneta, T., Sugimura, K., Takahashi, J., Fukumoto, Y., Takahashi, S., Shimokawa, H., 2014. Evidence for brain activation in patients with Takotsubo Cardiomyopathy. Circ. J. 78, 256–258.
Templin, C., Ghadri, J.R., Diekmann, J., Napp, L.C., Bataiosu, D.R., Jaguszewski, M., Cammann, V.L., Sarcon, A., Geyer, V., Neumann, C.A., Seifert, B., Hellermann, J., Schwyzer, M., Eisenhardt, K., Jenewein, J., Franke, J., Katus, H.A., Burgdorf, C., Schunkert, H., Moeller, C., Thiele, H., Bauersachs, J., Tschope, C., Schultheiss, H.P., Laney, C.A., Rajan, L., Michels, G., Pfister, R., Ukena, C., Bohm, M., Erbel, R., Cuneo, A., Kuck, K.H., Jacobshagen, C., Hasenfuss, G., Karakas, M., Koenig, W., Rottbauer, W., Said, S.M., Braun-Dullaeus, R.C., Cuculi, F., Banning, A., Fischer, T.A., Vasankari, T., Airaksinen, K.E., Fijalkowski, M., Rynkiewicz, A., Pawlak, M., Opolski, G., Dworakowski, R., MacCarthy, P., Kaiser, C., Osswald, S., Galiuto, L., Crea, F., Dichtl, W., Franz, W.M., Empen, K., Felix, S.B., Delmas, C., Lairez, O., Erne, P., Bax, J.J., Ford, I., Ruschitzka, F., Prasad, A., Luscher, T.F., 2015. Clinical features and outcomes of Takotsubo (Stress) Cardiomyopathy. N. Engl. J. Med. 373, 929–938.
Templin, C., Hanggi, J., Klein, C., Topka, M.S., Hiestand, T., Levinson, R.A., Jurisic, S., Luscher, T.F., Ghadri, J.R., Jäncke, L., 2019. Altered limbic and autonomic processing supports brain-heart axis in Takotsubo syndrome. Eur. Heart J. 40, 1183–1187.
Tzourio-Mazoyer, N., Landeau, B., Papathanassiou, D., Crivello, F., Etard, O., Delcroix, N., Mazoyer, B., Joliot, M., 2002. Automated anatomical labeling of activations in SPM using a macroscopic anatomical parcellation of the MNI MRI single-subject brain. NeuroImage 15, 273–289.
White, S.F., Geraci, M., Lewis, E., Leshin, J., Teng, C., Averbeck, B., Meffert, H., Ernst, M., Blair, J.R., Grillon, C., Blair, K.S., 2017. Prediction error representation in individuals with Generalized Anxiety Disorder during passive avoidance. Am. J. Psychiatry 174, 110–117.
Wittstein, I.S., Thiemann, D.R., Lima, J.A.C., Baughman, K.L., Schulman, S.P., Gerstenblith, G., Wu, K.C., Rade, J.J., Bivalacqua, T.J., Champion, H.C., 2005. Neurohumoral features of myocardial stunning due to sudden emotional stress. N. Engl. J. Med. 352, 539–548.
Yarkoni, T., Poldrack, R.A., Nichols, T.E., Van Essen, D.C., Wager, T.D., 2011. Large-scale automated synthesis of human functional neuroimaging data. Nat. Methods 8, 665–670.
Zigmond, A.S., Snaith, R.P., 1983. The hospital anxiety and depression scale. Acta Psychiatr. Scand. 67, 361–370.